International Journal of Mass Spectrometry 296 (2010) 15–20

Contents lists available at ScienceDirect

International Journal of Mass Spectrometry

journal homepage: www.elsevier.com/locate/ijms

Improvement of the resonance ionization mass spectrometer performance for precise isotope analysis of krypton and xenon at the ppt level in argon

Yoshihiro Iwata[a,*], Chikara Ito[a], Hideki Harano[b], Takafumi Aoyama[c]

[a] Experimental Fast Reactor Department, Oarai Research and Development Center, Japan Atomic Energy Agency, 4002 Narita, Oarai, Ibaraki 311-1393, Japan
[b] National Institute of Advanced Industrial Science and Technology, Central 2, 1-1-1 Umezono, Tsukuba, Ibaraki 305-8568, Japan
[c] Research Institute of Nuclear Engineering, University of Fukui, 3-9-1 Bunkyo, Fukui 910-8507, Japan

ARTICLE INFO

Article history:
Received 5 February 2010
Received in revised form 8 July 2010
Accepted 12 July 2010
Available online 17 July 2010

Keywords:
Resonance ionization mass spectrometry
Failed fuel detection and location (FFDL)
Photoelectron
Neutralization apparatus
Brewster window
Electrode with a slit

ABSTRACT

Resonance ionization mass spectrometry (RIMS) is an effective method for the isotope analysis of trace elements in terms of its insensitivity to isobaric interferences. In view of this advantage, RIMS has been proposed for application to the failed fuel detection and location (FFDL) system of the fast reactor. The principle of the FFDL technique using RIMS involves the isotope analysis of krypton (Kr) and xenon (Xe) with concentrations as low as parts-per-trillion (ppt) in argon (Ar). The precise detection of Kr and Xe isotopes at such low concentrations level is often difficult because of the existence of Ar^+ and Ar_2^+ ions caused by photoelectrons generated in the vacuum chamber. We show that using both a combination of a neutralization apparatus and a Brewster window, and an electrode with a slit in the ion acceleration region of the time-of-flight mass spectrometer (TOF-MS), helps decrease the effect of Ar^+ and Ar_2^+ ions, giving improved reliability of the FFDL system using RIMS.

1. Introduction

Recently, the analysis technique of trace substances has become indispensable in areas such as environmental science, cosmochemistry and nuclear engineering. Among the wide variety of analytical methods in existence, resonance ionization mass spectrometry (RIMS) is a relatively new method well suited for the isotope analysis of trace elements in terms of its insensitivity to isobaric interferences [1]. RIMS is the combination of resonance ionization spectroscopy (RIS) and mass spectrometry (MS), RIS being the resonance excitation of specific atoms with a monochromatic laser (or lasers in case of two or more excited states used) followed by ionization from the excited state with the same or another laser. An electric field pulse is sometimes used instead to ionize the Rydberg atoms [2,3]. Selective ionization of a particular element avoids the effect of isobars.

In view of this advantage, RIMS has been proposed for application to the failed fuel detection and location (FFDL) system of the fast reactor [4]. In existing reactors, many types of safety equipment are installed based on the concept of defense in depth. To ensure safety operation and a high plant availability of the fast reactors, it is necessary to set up a system for immediate and precise detection of fuel failures (FFD: fuel failure detection) when they occur, and for subsequent identification of the failed fuel location (FFDL) to reduce radiation exposure from fission products (FPs) in the failed pin. There are several FFD methods such as the delayed neutron method to detect delayed neutrons emitted from FPs, and the precipitator method or γ-ray spectrometry to measure FPs in the cover gas. As for FFDL techniques, also are proposed some effective methods including the sipping method used in the experimental fast reactor Joyo and the selector valve method, among which the gas tagging method is currently employed in the prototype Japanese fast breeder reactor Monju. The general principle of the gas tagging method shown in Fig. 1 is summarized as follows:

(a) Krypton and Xe gases of different isotopic compositions are loaded into fuel pins of as many as several hundred different fuel assemblies. Fuel pins in the same assembly have the same isotope abundance of Kr and Xe.
(b) In case of fuel failure, a partial amount of leaked Kr and Xe tag gas, together with FP, is quickly transported to the Ar cover gas region without any reaction with liquid sodium.
(c) Isotope analysis of Kr and Xe in the cover gas makes it possible to identify the assembly containing the failed pin.

Although depending on the cover gas volume and other conditions of fast reactors, typically the isotope analysis of Kr and Xe is required at concentrations as low as parts-per-trillion (ppt) in

* Corresponding author. Tel.: +81 29 267 4141; fax: +81 29 267 7481.
E-mail address: iwata.yoshihiro@jaea.go.jp (Y. Iwata).

1387-3806/$ – see front matter © 2010 Elsevier B.V. All rights reserved.
doi:10.1016/j.ijms.2010.07.014

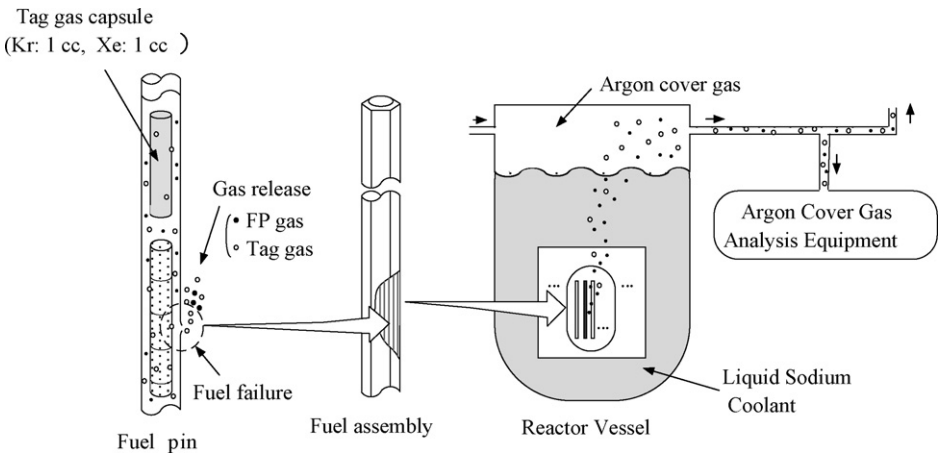

Fig. 1. Schematic diagram of the gas tagging method for the FFDL system.

Ar. The precision of the isotope analysis needed is determined by the difference of the isotopic compositions of Kr and Xe tag gases loaded into fuel pins in different fuel assemblies. Referring to the case in Monju with about two hundred kinds of fuel assemblies, this difference is designed to be about 20–30%. Considering that the identification of the corresponding failed fuel assembly involves the error in the tag gas fabrication and one caused by change in isotopic compositions during fuel burn-up, the order of one percent or better needs to be accomplished for the precision of the isotope analysis of Kr and Xe to allow for other possible errors to some extent.

The characteristic of RIMS to obtain a high signal-to-noise (S/N) ratio by selective photoionization of a specific element permits the direct measurement of Kr and Xe tag gas at the ppt level with high accuracy. Compared to other methods like the one adopted in Monju of increasing the tag gas concentration up to an order of parts-per-million (ppm) followed by double-focusing mass spectrometry, the fact that additional procedures are not needed in the RIMS method reduces the measurement time as well simplifying the FFDL system.

Even though RIMS is insensitive to unwanted atoms or molecules, precise detection of Kr and Xe isotopes (Kr isotopes in particular), to the targeted concentration ppt level is often complicated by Ar^+ and Ar_2^+ ions produced by photoelectrons generated in the vacuum chamber.

In this paper, we report on the improvement of our RIMS device for an FFDL system which involves decreasing the effect of Ar cover gas-originated ions by using both a combination of a neutralization apparatus and a Brewster window, and an electrode with a slit in the ion acceleration region of the time-of-flight mass spectrometer (TOF-MS). In addition, the precision of the isotope analysis was estimated for both Kr and Xe by measurements of 100 ppt of Kr and Xe containing Ar standard gas over about 1000 s for assessment of the reliability of RIMS.

2. Experimental setup

2.1. RIS scheme of Kr and Xe

Several resonance ionization schemes have been investigated for Kr and Xe, including single and two-photon resonance excitations [5–7]. Since the noble gas atoms require large energy (around 10 eV or more) for the transition from the ground state, it is rather difficult to obtain sufficient laser output by commercially available lasers with corresponding single-photon resonance wavelength of shorter than 200 nm. We chose therefore the resonant "2 + 1" transition, two-photon resonance excitation followed by single-photon ionization at the same wavelength, for the resonance ionization of Kr and Xe using 216.67 and 256.02 nm wavelength in vacuum, respectively, as shown in Fig. 2(a).

2.2. Instrument description

A schematic diagram of the experimental apparatus is illustrated in Fig. 2(b); it consists of four parts: (1) a tunable pulsed laser system, (2) a system to introduce gas, (3) a reflectron-type TOF-MS, and (4) a data acquisition system. This basic design was previously reported for the detection of Xe [8].

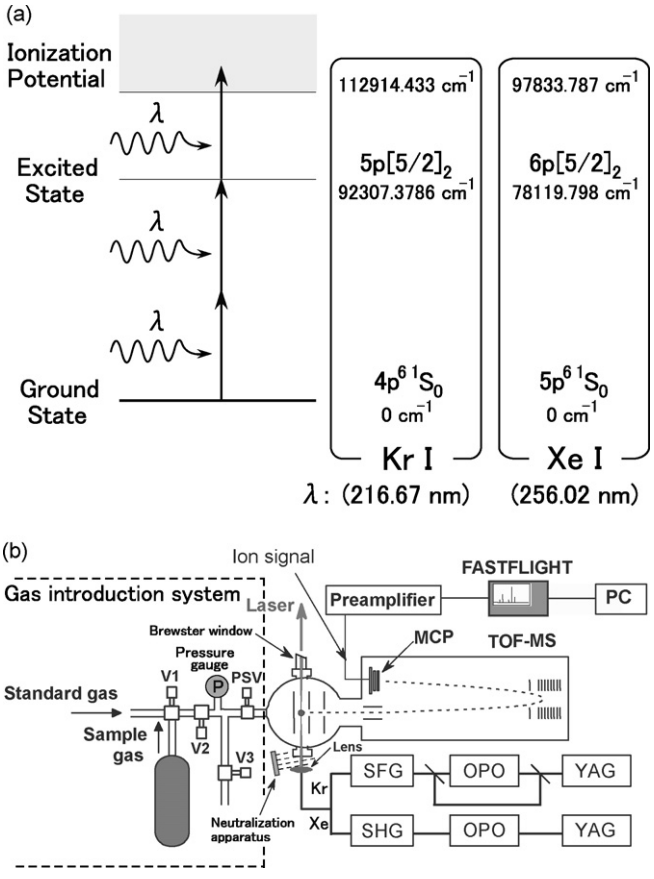

Fig. 2. Experimental conditions in this work: (a) resonance ionization scheme of Kr and Xe used in this work, and (b) schematic diagram of the experimental apparatus. The value of each energy level in (a) is cited from [7].

Our tunable pulsed laser system by Continuum, Inc. can produce a ~5 mJ/pulse of 216.67 nm for Kr and nearly a 10 mJ/pulse of 256.02 nm for Xe, both at a repetition rate of 10 Hz with a ~10 ns pulse width. It consists of a Powerlite Precision II 9010 Nd:YAG, a Sunlite EX optical parametric oscillator (OPO), and an FX-UV sum frequency generation (SFG) system for 216.67 nm or an FX-1 second harmonic generation (SHG) system for a wavelength of 256.02 nm. To generate the 216.67 nm light, the OPO output at 557 nm, pumped by the third harmonic of the Nd:YAG laser (355 nm) is sum-frequency mixed with the remaining 355 nm light. For the 256.02 nm light, the OPO output wavelength is tuned to 512 nm and frequency-doubled by the SHG crystal. The UV laser beam is then focused by a plano-convex lens with a focal length f of 300 mm to the ionization region in vacuum where the introduced gas is photoionized. For an assumed Gaussian beam, the beam diameter D at the focal point is calculated to be

$$D = \frac{4\lambda f}{\pi d} \simeq \begin{cases} 17\,\mu\text{m} & (\lambda = 216.67\,\text{nm}) \\ 20\,\mu\text{m} & (\lambda = 256.02\,\text{nm}) \end{cases}, \quad (1)$$

where λ and d = 5 mm are the laser wavelength and the diameter of the collimated beam before focusing through the lens, respectively. The spherical aberration of the lens is negligibly small in this setup. A neutralization apparatus and a Brewster window are placed in the configuration shown in Fig. 2(b), the purpose of which is described in Section 3.

An R.M. Jordan C-211 pulsed supersonic valve (PSV) is used to introduce gas as a pulsed beam to improve sensitivity without increasing the required vacuum pumping. It operates on the magnetic beam repulsion principle [9] by passing a high pulsed current through two parallel beam conductors in a hairpin configuration. The resulting gas jet of 55 μs pulse width at 10 Hz is synchronized with the laser pulse. The desired concentration of Kr and Xe in Ar introduced by the PSV is prepared by diluting the 100 ppm of Kr and Xe containing Ar gas with pure Ar gas by use of mass flow controllers. A three-way valve (V1) is placed to select either the standard gas or the sample gas for measurement, but only the standard gas of known concentration is used in this work. Measurement of the sample gas will be performed for unknown samples such as an Ar cover gas collected in the actual fast reactor.

The generated ions are accelerated up to about 1 keV and mass analyzed by an R.M. Jordan reflectron-type TOF-MS. The TOF-MS is equipped with a microchannel plate (MCP) to detect ions as an amplified voltage.

The MCP output is amplified by a wideband preamplifier (Model 5185) and then stored in a FASTFLIGHT digital signal averager, both devices EG&G Instruments. The FASTFLIGHT device digitizes the input signal at 500 MHz sampling rate and averages the resulting records to form a TOF spectrum which is displayed in the computer. The output voltage in the FASTFLIGHT device has to be less than 1 V.

3. Improved methods

Selective ionization is the main feature of RIMS; however, actual experimental data indicate the existence of both Ar and Ar_2 non-resonant ionization. Fig. 3 shows an example of the TOF spectrum measured for pure Ar gas before adopting the improved methods described below. The laser wavelength was tuned to the resonance wavelength of Kr atoms (216.67 nm).

The observed three peaks correspond to the m/z values of around 20, 40 and 80, those for Ar^{2+}, Ar^+ and $Ar_2{}^+$, respectively, and the same holds for the non-resonant wavelength. Among these three, Ar^+ ions may cause the saturation of the output voltage to deteriorate the MCP detector. The Ar^+ peak intensity is known to vary almost in proportion to the laser energy by the previous work [8]. On the other hand, $Ar_2{}^+$ions unfortunately interfere with ^{80}Kr, a

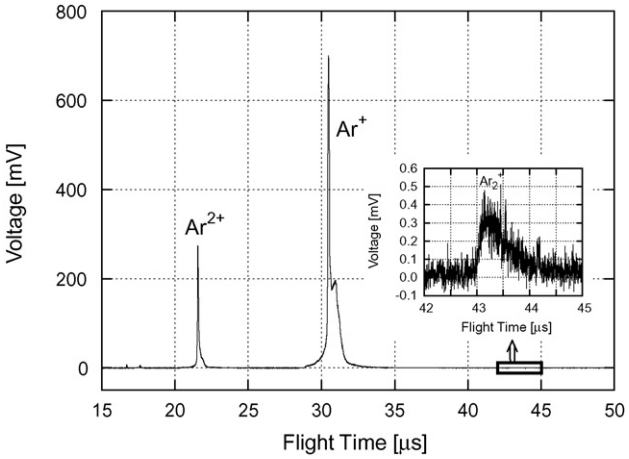

Fig. 3. Example of the TOF spectrum measured for pure Ar gas before adopting the improved methods.

suitable nuclide for tag gas. Each peak has a considerably long tail in longer time region, or higher mass region, which means time delay in ionization instead of photoionization during laser irradiation. This phenomenon probably comes from the fact that the photoelectrons generated by reflected or scattered light hitting the electrodes or surface of the vacuum chamber can non-resonantly ionize Ar atoms and Ar_2 molecules.

For decreasing the adverse effects of these ions, the following two methods are considered for application in terms of reducing the amount of photoelectron and limiting the number of these ions reaching the detector.

- Neutralization apparatus and Brewster window

  The combination of a neutralization apparatus and a Brewster window, as shown in Fig. 2(b), is effective in decreasing the number of photoelectrons. The neutralization apparatus removes any charged particles on the targeted surface by producing positive and negative ions to neutralize it. A Kasuga Electric Works Ltd. model KD-110 is placed about 10 cm away from the viewport window at the entrance side of the vacuum tube to avoid attachment of any charged dust during measurement. The Brewster window mounted at the exit of the vacuum tube in the laser irradiation direction uses a window tilted at a Brewster angle θ_B to prevent reflection of p-polarized light. It is made of quartz with a refractive index n_q of 1.459, so the Brewster angle is approximately $\theta_B = \tan^{-1}(n_q) \simeq 56^\circ$. These charged dust and reflected p-polarized light will otherwise generate photoelectrons.
- Electrode with a slit

  An electrode with a slit instead of a circular hole is proposed as the center of the ion acceleration electrodes to limit the Ar^+ and $Ar_2{}^+$ ions reaching the detector without loss of the Kr^+ and Xe^+ ion signals. Although the center electrode has a circular hole in the typical TOF-MS for extracting as many ions as possible, a slit is much more suited to the RIMS setup because Kr^+ and Xe^+ resonant ions are created within the laser irradiation region, but Ar^+ and $Ar_2{}^+$ non-resonant ions can be generated away from the laser path as illustrated in Fig. 4. In this work, the size of the slit was determined to be 1 mm × 10 mm taking into account that the electrode used so far had a circular hole of 12.7 mm diameter and the laser spot diameter at the focal point given by Eq. (1) is sufficiently smaller than 1 mm. The electrode with the circular hole has a metallic mesh with 20–50 μm thick wires placed at 0.5 mm intervals, but the electrode with the slit has no meshes.

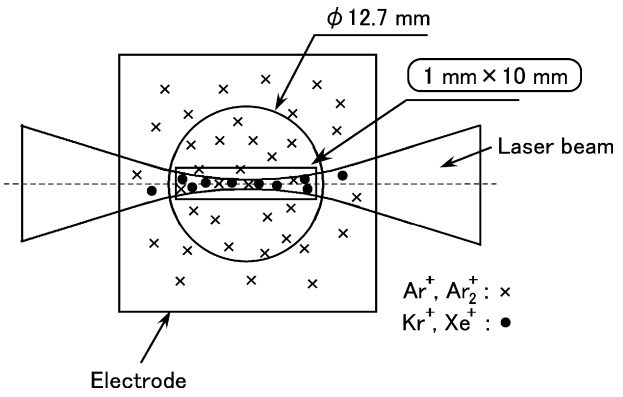

Fig. 4. Comparison of two types of electrode structures with a slit (1 mm × 10 mm) and a circular (Ø 12.7 mm) hole.

4. Results and discussion

The Ar^+ and Ar_2^+ ions described in the previous section more seriously affect Kr than Xe because of the shorter laser wavelength (216.67 nm for Kr and 256.02 nm for Xe), as well as Ar_2 interference with Kr. Measured results using the proposed improved methods are therefore reported in this paper mainly for the laser wavelength of corresponding to resonance ionization of Kr.

4.1. Effect of a neutralization apparatus and a Brewster window

To observe the effect of a neutralization apparatus and a Brewster window, we performed 10-min measurements of pure Ar gas under the following conditions:

(i) The normal viewport windows are mounted at the entrance and exit of the vacuum tube in the laser irradiation direction without a neutralization apparatus or a Brewster window. Each window is coated with a dielectric multilayer coating (antireflection coating) for the resonance wavelength of Kr (217 nm) or Xe (256 nm) so that the nominal reflectivity is below 1% with the undamaged coating.
(ii) The viewport window at the exit side is replaced with an uncoated Brewster window and a neutralization apparatus is added near the entrance of the tube as shown in Fig. 2(b).

Experimental results are given in Fig. 5, where "Before" and "After" correspond to the conditions of (i) and (ii) above, respectively. The preamplifier gain was set to 10 and the laser output was around 5 mJ/pulse for both of these conditions. The measurement with a neutralization apparatus and a Brewster window was done after that without them. Even though the amount of the photoelectron has a tendency to increase as the damage on the window builds up with prolonged laser irradiation, a remarkable reduction to about one-third or less was observed for all three ions: Ar^{2+}, Ar^+ and Ar_2^+.

4.2. Effect of an electrode with a slit

Before the actual measurements, the vertical DC offset of the FASTFLIGHT device was first optimized to reduce background noise without decreasing the incoming single ion pulse. We found the optimized vertical offset for the preamplifier gain of 100 to be +5 mV, from which the optimized vertical offset of +0.5 mV was assumed for the preamplifier gain of 10. This procedure was not performed in the measurement described in Section 4.1.

After the optimization of the vertical offset to improve the S/N ratio, several measurements were carried out under the following conditions to evaluate the effect of an electrode with a slit:

(I) The center electrode has a Ø 12.7 mm circular hole and the preamplifier gain is set to 10 (same as (ii) in Section 4.1).
(II) The center electrode is replaced with one having a 1 mm × 10 mm slit. Other conditions remain the same as (I).
(III) The preamplifier gain is increased to 100. Other conditions remain the same as (II).

A neutralization apparatus and a Brewster window were applied and the laser output was adjusted to 3.3–3.4 mJ/pulse throughout the measurements. A new viewport window was mounted at the entrance of the vacuum tube in each measurement to avoid any difference arising from the different surface condition of the window described in Section 4.1. Each measurement was performed over 1024 s.

A comparison of the results using 100 ppt of Kr containing Ar standard gas is shown in Fig. 6 for the experimental conditions of (I) denoted by "Circle", and (II) denoted by "Slit". A significant decrease of Ar^{2+} and Ar^+ ion yields to nearly about 10% was successfully achieved with a slight increase, not a decrease, of Kr ion signals. The increase of 10–20% was reproducible for each Kr isotope in spite of the smaller ion extraction region, or hole area, as shown in Fig. 4. This may be attributable to the following two factors: (1) decrease in the space-charge effect to cause divergence of ions to decrease the detection efficiency by reducing the amount of the extracted Ar and Ar_2 ions, and (2) increase in the ion transmission efficiency by the absence of the metallic mesh on the electrode with a slit. The space-charge effect may distort the TOF spectrum, but the obtained results do not show any difference in the shape of

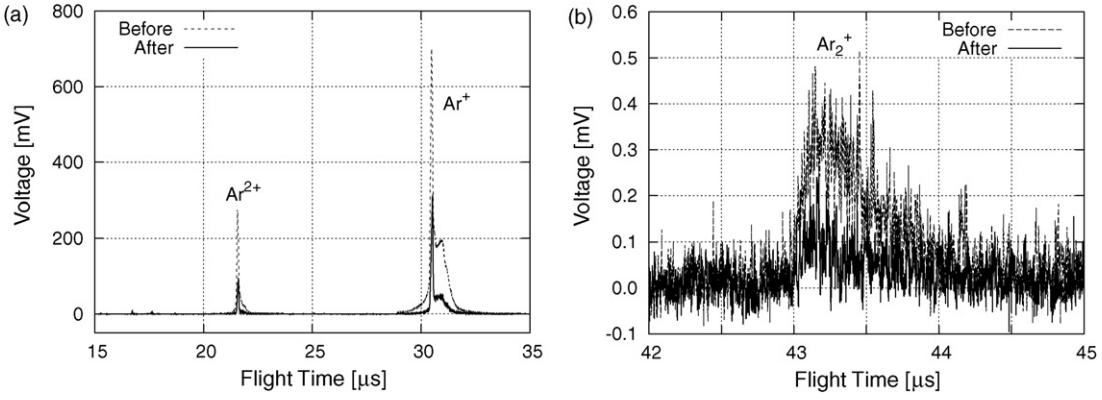

Fig. 5. Obtained TOF spectrum by the measurements of pure Ar gas for observation of the effect of a neutralization apparatus and a Brewster window: (a) reduction of Ar^{2+} and Ar^+ ion yields, and (b) reduction of Ar_2^+ ion yield. See text for the meaning of "Before" and "After".

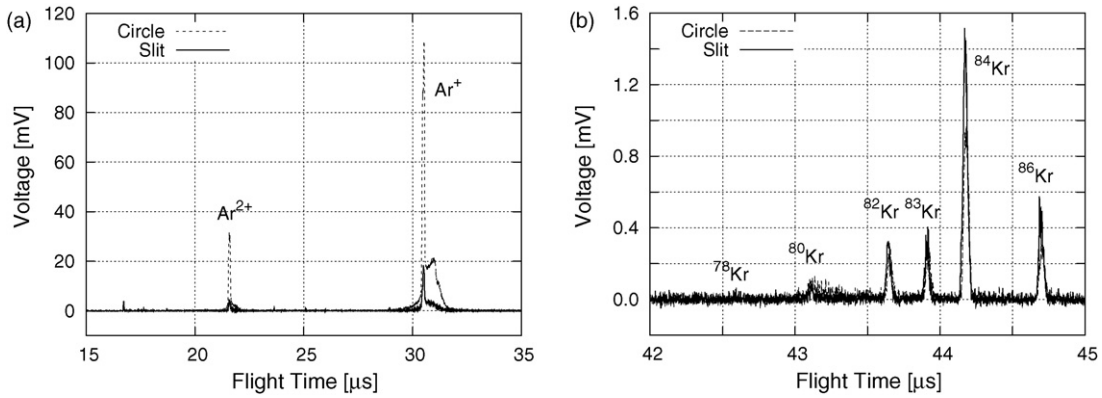

Fig. 6. Obtained TOF spectrum by the measurements of 100 ppt of Kr containing Ar standard gas for observation of the effect of an electrode with a slit: (a) reduction of Ar^{2+} and Ar^{+} ion yields, and (b) slight increase of Kr^{+} resonant ion signals. See text for the meaning of "Circle" and "Slit".

the spectrum. The latter would rather affect the measured results, meaning that changes in the electric field of the ionization region without any meshes on the electrode are small if the electrode with a slit is used, and that the loss of the number of ions hitting the mesh wires is relatively large.

Now that the Ar^{+} output voltage could be successfully reduced to far below 100 mV, as shown in Fig. 6(a), the preamplifier gain was increased up to 100 for precise measurement of the influence of the Ar_2 interference. Fig. 7 gives the results using (a) 100 ppt of Kr containing Ar standard gas, and (b) pure Ar gas under the condition of (III). The mass peak of ^{80}Kr, corresponding to the nuclide concentration of ~2 ppt, was clearly observed without any obvious Ar_2^{+} peak. It indicates, as a result, that the Ar dimer interference with ppt detection of Kr, ^{80}Kr in particular, was successfully excluded without any loss of Kr ion signals by the adoption of both a combination of a neutralization apparatus and a Brewster window, and an electrode with a slit, supposing that a new viewport window is mounted at the entrance of the vacuum tube in each measurement.

4.3. Precision of the isotope analysis

The precision of the isotope analysis was estimated for both Kr and Xe by measuring Ar standard gas containing 100 ppt of Kr and Xe under the condition of (III) described in Section 4.2 but with the viewport window damaged to some degree. The laser output at the time of measurement was around 2 mJ/pulse for Kr and 8 mJ/pulse for Xe. Each measurement was taken over a period of 1024 s and the data were divided into ten equal time intervals (102.4 s). The measurement time of about 1000 s is set to be a target in this work as the present FFDL method adopted in Monju usually takes about the total of 10 h for the isotope analysis. Reduction of the measurement time for the isotope analysis is highly significant in the FFDL system. The ratio of the measured ion yield, defined as the integrated MCP output voltage over the corresponding TOF region, for each Kr or Xe isotope to that of ^{84}Kr or ^{129}Xe, respectively was obtained in each 102.4-s measurement data, whose error was calculated by using the ten data under equal conditions. This ratio was then divided by that expected by the natural abundance ratio of each Kr or Xe isotope to estimate deviation of the obtained value from unity.

Table 1 summarizes the measured results with the 1σ error for each Kr and Xe isotope. The precision of the isotope analysis seems to be the order of tens of percent for ppt level detection of Kr and slightly better for Xe, and is mainly dominated by statistical errors. The precision would be worse for the detection of ^{80}Kr if Ar_2 interferes with ^{80}Kr, but we could successfully reduce the effect of the Ar_2 interference to a negligible extent as can be seen in Fig. 7. A single ion counting technique needs to be established for exact estimation of the analytical precision, which will be done in the future. Systematic errors caused by laser output fluctuation is negligible because the fluctuation affects each Kr or Xe isotope equally so that the ratio of the measured ion yield between two isotopes of the same element remains almost unchanged.

Although the required precision is dependent on the design of the fast reactor, an order of a percent or better is probably needed for detection of Kr and Xe to the ppt level in order to discriminate between several hundred fuel assemblies with different mixture ratios of Kr and Xe isotopes. Therefore, the analytical precision of one to two orders of magnitude better than at present should be achieved to meet the demand, which is thought to be solved by the improvement of the detection efficiency. From this point of view, utilization of a linear-type TOF-MS instead of a reflectron-type one would be effective in addition to the increase of the laser output.

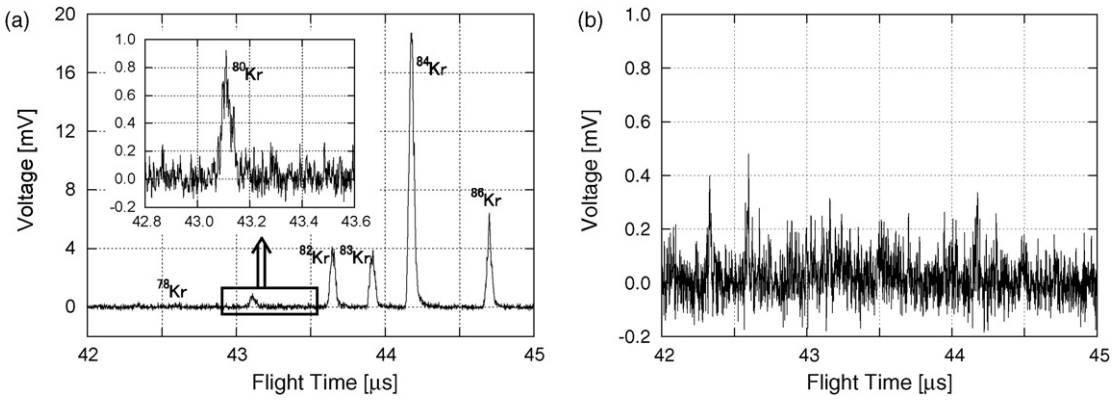

Fig. 7. Measured results for an electrode with a slit (1 mm × 10 mm) under the preamplifier gain of 100: (a) 100 ppt of Kr containing Ar standard gas, and (b) pure Ar gas.

Table 1
Analytical precision of the isotope ratio obtained with 100 ppt of Kr and Xe containing Ar standard gas.

Nuclide		Concentration [ppt]	Precision
Kr	^{78}Kr	0.355	0.90 ± 1.97
	^{80}Kr	2.286	0.24 ± 0.39
	^{82}Kr	11.593	1.04 ± 0.11
	^{83}Kr	11.500	1.07 ± 0.07
	^{84}Kr	56.987	(1)
	^{86}Kr	17.279	1.03 ± 0.06
	Total	100	–
Xe	^{124}Xe	0.0952	0.85 ± 0.69
	^{126}Xe	0.0890	0.54 ± 0.58
	^{128}Xe	1.9102	1.17 ± 0.11
	^{129}Xe	26.4006	(1)
	^{130}Xe	4.0710	0.94 ± 0.03
	^{131}Xe	21.2324	0.96 ± 0.05
	^{132}Xe	26.9086	0.97 ± 0.02
	^{134}Xe	10.4357	0.99 ± 0.03
	^{136}Xe	8.8573	0.91 ± 0.05
	Total	100	–

The expected mass resolution would become worse, but is enough for the detection of Xe and a bit lighter element of Kr with increased accelerating voltage in the ionization region, if necessary [6,10]. An atom buncher may also help increase the detection efficiency, which is a cold trap to capture gas atoms evaporated by the following heating laser irradiation [11], but additional cryogenic sample concentrator has to be attached in the vacuum tube.

5. Conclusion

Precise isotope analysis to the ppt level of Kr and Xe in Ar has been developed. However, two problems remain; namely, the saturation of the output voltage by Ar^+ ions, and Ar_2 interference mainly with ^{80}Kr. We proposed the following two methods to decrease the adverse effects of Ar^+ and $Ar_2{}^+$ ions:

- Neutralization apparatus and a Brewster window to reduce the number of photoelectrons.
- Electrode with a slit to limit the generated Ar^+ and $Ar_2{}^+$ ions reaching the MCP detector without any loss of Kr^+ and Xe^+ ion signals.

The obtained measurement results using 100 ppt of Kr containing Ar standard gas show that the Ar^+ ion yield could be successfully decreased by one to two orders of magnitude, and that the mass peak of ^{80}Kr corresponding to its nuclide concentration of ~2 ppt was clearly observed without any obvious $Ar_2{}^+$ peak under the viewport window undamaged. The effect of Ar^+ and $Ar_2{}^+$ ions is much smaller for the detection of Xe.

Additional measurements of Kr and Xe containing Ar standard gas were taken over a period of 1024 s to estimate the precision of the isotope analysis. According to the obtained measurement data, the precision seems to be the order of tens of percent for ppt level detection of Kr, and slightly better for Xe, which is mainly dominated by statistical errors. A single ion counting technique needs to be established for exact estimation of the analytical precision. Utilization of a linear-type TOF-MS or an atom buncher to increase the detection efficiency would improve the reliability of the FFDL system using RIMS.

Acknowledgements

The authors are grateful to T. Arima for his technical assistance during the experiments including operation of the laser system. We also want to thank Y. Araki, K. Watanabe and T. Iguchi for helpful comments and advice.

References

[1] M.G. Payne, L. Deng, N. Thonnard, Rev. Sci. Instrum. 65 (1994) 2433.
[2] R. Zilliacus, J. Likonen, Appl. Spectrosc. 46 (1992) 1828.
[3] T. Aoyama, C. Ito, K. Okazaki, H. Harano, K. Watanabe, T. Iguchi, J. Nucl. Sci. Technol. Suppl. 5 (2008) 1.
[4] K. Watanabe, T. Iguchi, T. Ogita, A. Uritani, H. Harano, J. Nucl. Sci. Technol. 38 (2001) 844.
[5] E.B. Saloman, Spectrochim. Acta B 46 (1991) 319.
[6] J.D. Gilmour, S.M. Hewett, I.C. Lyon, M. Stringer, G. Turner, Meas. Sci. Technol. 2 (1991) 589.
[7] NIST Atomic Spectra Database, http://physics.nist.gov/PhysRefData/ASD/index.html.
[8] H. Harano, C. Ito, K. Watanabe, T. Iguchi, Int. J. Appl. Electrom. Mech. 14 (2001/2002) 307.
[9] W.R. Gentry, C.F. Giese, Rev. Sci. Instrum. 49 (1978) 595.
[10] S.A. Crowther, R.K. Mohapatra, G. Turner, D.J. Blagburn, K. Kehm, J.D. Gilmour, J. Anal. At. Spectrom. 23 (2008) 938.
[11] G.S. Hurst, M.G. Payne, R.C. Phillips, J.W.T. Dabbs, B.E. Lehmann, J. Appl. Phys. 55 (1984) 1278.